Cell Tissue Res (1990) 262:307–313

Cell and Tissue Research

© Springer-Verlag 1990

Contralateral projections of the optic tectum in the zebra finch (*Taenopygia guttata castanotis*)

Hans-Joachim Bischof and Jutta Niemann

Universität Bielefeld, Lehrstuhl für Verhaltensphysiologie, Bielefeld, Federal Republic of Germany

Accepted July 4, 1990

Summary. Efferent projections of the optic tectum of zebra finches were investigated by injection of the radioactive anterograde tracer ^{3}H-proline. In addition to a variety of ipsilateral projections, some contralateral connections were found. Quantitative evaluation of the recrossing tecto-rotundal and nucleus subpraetectalis/nucleus interstitio-praetecto-subpraetectalis projection revealed that these connections are much stronger than previously believed. In contrast, the tecto-tectal projection is very weak, as has been shown previously. Further support for this comes from results obtained using injections of retrograde tracers. The role of the different projections in conveying information from the ipsilateral eye to the ectostriatum, the telencephalic end-station of the tectofugal pathway, is discussed.

Key words: Visual system, avian – Tectum opticum – Tectofugal pathway – Recrossing fibers – ^{3}H-proline, labeling – Retrograde tracers – *Taeniopygia guttata castanotis* (Aves, Passeriformes)

The optic tectum is a highly developed part of the tectofugal pathway of birds, leading from the eye via the optic tectum of the contralateral side to the nucleus rotundus and then to the telencephalic target of this pathway, the ectostriatum. Until recently, the tectofugal pathway was considered to process information mainly from the contralateral eye, because of the lack of ipsilaterally projecting ganglion cell fibers in adult birds (McLoon and Lund 1982; O'Leary et al. 1983; Weidner et al. 1985; Bagnoli et al. 1980). A few recrossing fibers were found that connected the two tecta or the tectum and nucleus rotundus of the contralateral side. These were thought to have little impact on processing of visual information (Benowitz and Karten 1976).

However, recent experiments from our laboratory have demonstrated that prominent responses to ipsilateral stimuli appear in the ectostriatum and that, under normal conditions, this ipsilateral response is largely suppressed by the activity of the contralateral eye (Engelage and Bischof 1988, 1989). If the contralateral eye is enucleated, the ipsilateral response of the ectostriatal neurons becomes nearly as large as the contralateral response in intact birds. Similarly, monocular deprivation studies (Herrmann and Bischof 1986a, b; Nixdorf and Bischof 1987) demonstrate that the effects of deprivation of one eye can be detected in both hemispheres. These findings show that a substantial amount of visual information crosses over to the ipsilateral hemisphere. We have therefore re-examined the efferent projections of the optic tectum of the zebra finch to evaluate the extent to which the tectum is connected to the contralateral hemisphere.

Send offprint requests to: Prof. Dr. H.-J. Bischof, Universität Bielefeld, Lehrstuhl Verhaltensphysiologie, Postfach 8640, 4800 Bielefeld 1, Federal Republic of Germany

Materials and methods

The experiments were performed on a total of 30 adult zebra finches of both sexes obtained from the Institute's stock. For quantitative evaluations only males were used. The birds were anesthetized by an injection of 0.05 ml Equithesin and mounted on a stereotaxic headholder especially designed for small birds (Bischof 1981).

Injections were made using a 1 µl microsyringe with a glass pipette (inner tip diameter ≈3–5 µm) glued to the tip of the injection needle. For tectal injections, the skull was opened dorsorostrally from the ear canal, and the spongious bone and second bone layer which covers the tectum, were removed. The glass pipette was then lowered into the tectum with the help of a micromanipulator under visual control. Rotundus injections were made stereotaxically. Coordinates (2.0 mm lateral, 2.6 mm anterior from the reference point, 5.0 mm depth measured from the brain surface) were derived from a stereotaxic atlas of the zebra finch brain (H.-J. Bischof and B. Nixdorf, unpublished).

Efferent projections

To demonstrate efferent projections, radioactively labeled proline (2,3,4,5-^{3}H-α-proline, NEN, 0.4 µC in 0.4 µl saline, 0.9%) was injected into the tectum. To assure equal distribution of the tracer over a large part of the tectum, the total amount of the tracer was injected in four 0.1 µl aliquots at different positions. This nor-

mally resulted in a rather uniform distribution of the tracer in about 2/3 of the stratum griseum centrale (SGC) of the tectum opticum.

The survival time of the animals was 14 days. Each bird was then decapitated, the brain quickly removed from the skull and immediately frozen on a cryostat specimen holder with dry ice. One day later, 30 µm sections were cut in the coronal plane. The sections were then melted onto microscope slides and immediately dried at 60° C to keep the liquid phase as short as possible. The next day, the sections were fixed with 4% formaldehyde for 1/2 h, defatted in an ascending alcohol series and dried in a drying cupboard overnight at 37° C.

The slides were then dipped into Kodak NTB2 emulsion (1:1 with distilled water) at 40° C under safelight conditions and hung in the dark to obtain an equal thickness of the emulsion. When dry, the slides were stored at 4° C in light-proof boxes for 14 days and then developed with Kodak D19 developer. Every third section was stained with hematoxylin, and all sections were coverslipped with Canada balsam.

The slides were examined by dark-field optics and the projections were identified using the stereotaxic atlasses of the pigeon (Karten and Hodos 1967), the canary (Stokes et al. 1972) and the zebra finch (H.-J. Bischof and B. Nixdorf, unpublished). The abbreviations were mainly derived from the atlas of Stokes et al. (1972) (see Abbreviation list in Fig. 3).

The density of silver grains induced by the transported radioactive proline was estimated by counting the grains on photographs of a given area (magnification 768 ×) within grids of 2 × 2 cm (26 × 26 µm). Counts were performed on at least 5 successive sections in at least 100 grid partitions. Alternatively, the luminance of a given area was measured using the spot measurement mode of the exposure meter of the photomicroscope (Zeiss Photomikroskop III with integrated camera). The diameter of the employed spot was 25 µm, about 1/20 of the diameter of the nucleus rotundus. As the exposure meter of the microscope had an unexact scale, the voltages representing the luminance were measured by an external voltage meter attached to the luminance measuring circuit of the microscope.

Two measurements were taken from each of at least 5 successive sections. significant luminance differences between different parts of nucleus rotundus were not detected. Relative densities were then calculated with the luminance of the nucleus rotundus ipsilateral to the injection set as 100%. This method was much faster than the grain counts and gave essentially the same results (see Table 2).

Afferent projections

Tecto-rotundal projections were confirmed by injections of either 30% horseradish peroxidase (HRP; Sigma; w/v) in 2% dimethylsulfoxide (DMSO), or 2% rhodamine isothiocyanate (RITC; Sigma, w/v) in 2% DMSO into the nucleus rotundus. The amount of tracer injected varied between 0.02 and 0.05 µl. This resulted in injection sites with diameters of 80 to 120 µm with diffusion zones of about the double size. Spreading of the tracer to regions outside nucleus rotundus was observed in some preparations. However, this most probably did not influence the results, as injections located around nucleus rotundus never caused the appearance of labeled neurons within the tectum opticum.

HRP-injected birds were deeply anesthetized with 0.03 ml Nembutal after 24 h, perfused with 0.9% saline followed by a mixture of 1.25% glutardialdehyde/1% paraformaldehyde in 0.1 M phosphate buffer (pH 7.4), and then by the same solution with 10% sucrose added. The brains were removed from the skull and stored overnight in the fixative-sucrose solution. The next day, 40 µm sections were cut on a freezing microtome. The sections were then processed using tetramethyle benzidine as chromogen according to the protocol of Mesulam (1978), mounted on gelatine-coated slides and counterstained with neutral red. Labeled neurons within the tecta were counted in every third section using dark-field optics.

RITC-injected birds were perfused after 24 h survival with 0.9% saline followed by 4% paraformaldehyde in phosphate buffer and by paraformaldehyde/10% sucrose. The brains were stored overnight in the same solution, and then 40 µm sections were cut on a freezing microtome. The sections were mounted onto slides, dried and coverslipped with Fluoromount. Sections were examined with a Zeiss fluorescence microscope. Adjacent sections were stained with cresyl violet to identify the labeled structures and to localize the injection site.

In one brain, all labeled neurons within the tecta were counted on every third section. In the other brains, samples from at least 10 sections were taken from the central part of the tectum using on ocular grid that covered an area of 400 × 400 µm (marked with asterisks in Table 3).

Results

Proline injections

As a result of proline injections into the optic tectum, a variety of brain areas were labeled mainly in the diencephalon, mesencephalon and brainstem (Table 1). Nineteen different structures were labeled ipsilaterally.

Table 1. Brain areas labeled by ^{3}H-proline injections into the optic tectum

Diencephalon	Ipsi-	Contra-	Bilateral
Rt			X
T			X
SRt	X		
DLL	X		
PV	X		
VLT	X		
GLv	X		
DLP	X		
Mesencephalon			
TeO		X	
AP			X
SP			X
IPS			X
LM	X		
GT	X		
PT	X		
Imc	X		
Ipc	X		
SLu	X		
ION	X		
Brainstem			
ICO	X		
PM	X		
PL	X		
RPO	X		
GCt	X		
FRL	X		
FRM		X	
PAP		X	
Pam		X	

Abbreviations: see Fig. 3

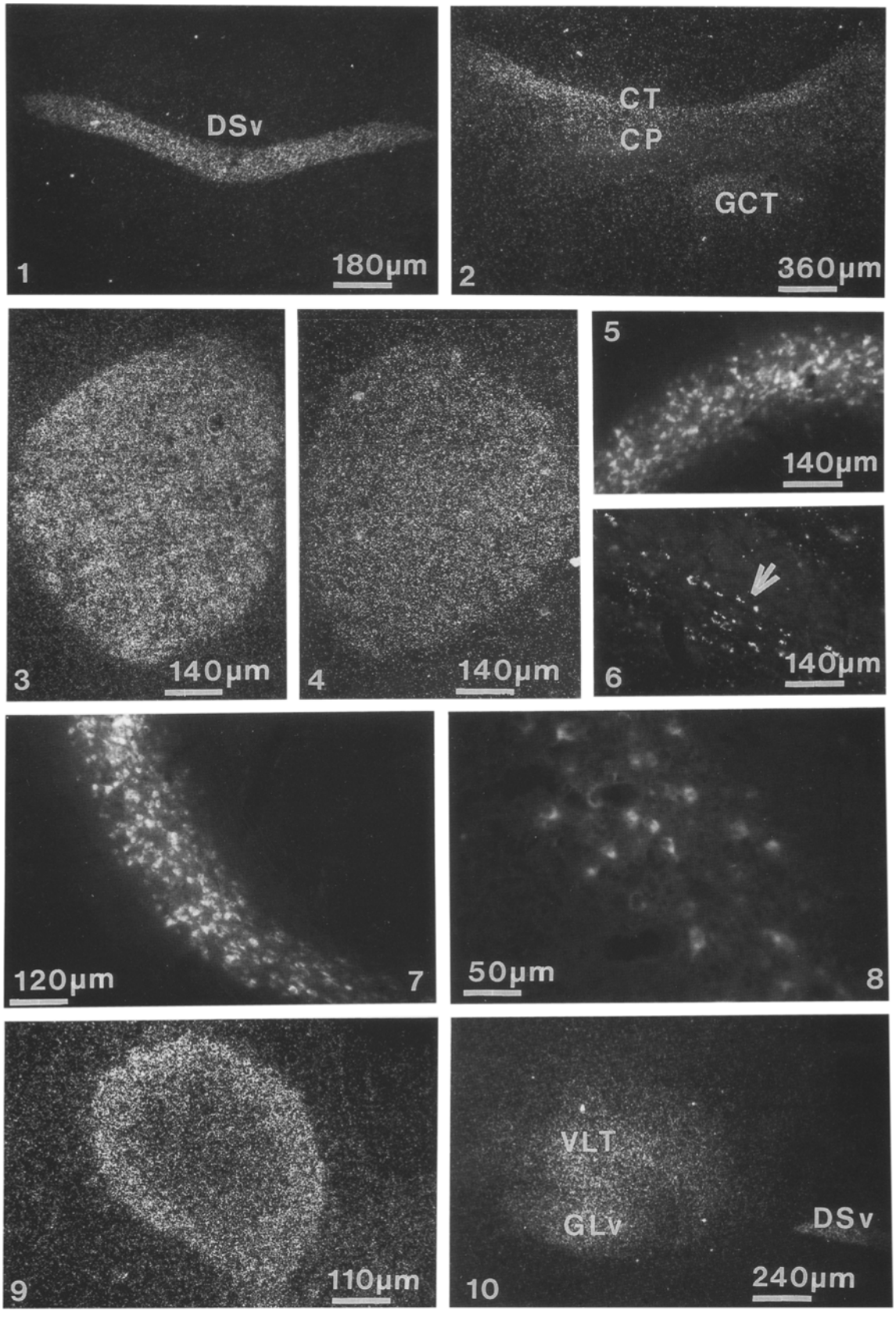

Fig. 1.1–10. Interhemispheric connections. *1.1* Decussatio supraoptica ventralis (*DSv*). ^{3}H-proline, tectum injection, dark field. *1.2* Commissura posterior (*CP*) and commissura tectalis (*CT*); *GCT* substantia grisea centralis. ^{3}H-proline, tectum injection, dark field. *1.3, 1.4* Nucleus rotundus ipsilateral (3) and contralateral (4) to the injection site. ^{3}H-proline, tectum injection, dark field. *1.5, 1.6* Ipsilateral tectal label after injection of RITC (5) and HRP (6) to nucleus rotundus. *Arrow* in (6) points to labeled neurons within the stratum griseum centrale (*SGC*). *1.7, 1.8* Ipsilateral (7) and contralateral (8) tectal label after injection of RITC into the nucleus rotundus. Note that the magnifications are different. *1.9* Nucleus praetectalis ipsilateral to the injection site. ^{3}H-proline, tectal injection, dark field. *1.10* Nucleus ventrolateralis thalami (*VLT*) and nucleus geniculatus lateralis, pars ventralis (*GLv*) ipsilateral to the injection site. *DSv* decussatio supraoptica ventralis. ^{3}H-proline, tectal injection, dark field

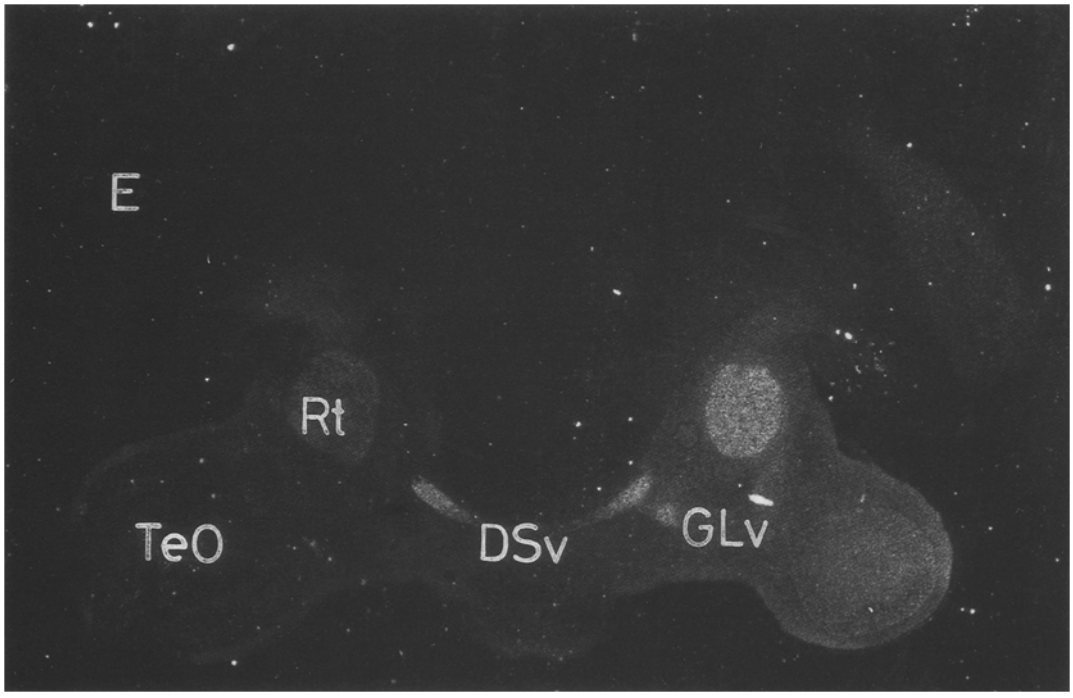

Fig. 2. Coronal section through a zebra finch brain. ^{3}H-proline injection to the right-side tectum. Abbreviations, see Fig. 3

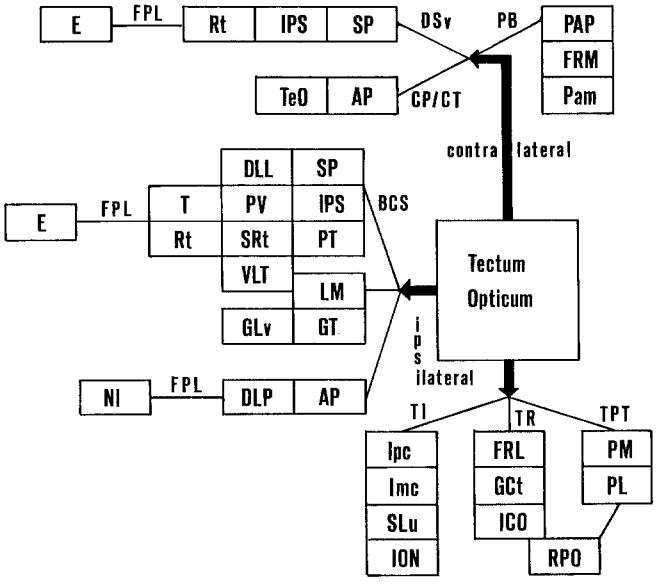

Fig. 3. Diagrammatic representation of efferent projections obtained in this study. *Abbreviations: AP* Area praetectalis; *BCS* Brachium colliculi superioris; *CP* Commissura posterior; *CT* Commissura tectalis; *DLP* N. dorsolateralis posterior thalami; *DLL* N. dorsolateralis anterior thalami, pars lateralis; *DSv* Decussatio supraoptica ventralis; *E* Ectostriatum; *FPL* Fasciculus prosencephali lateralis; *FRL* Formatio reticularis lateralis; *FRM* Formatio reticularis medialis; *GCT* Substantia grisea centralis; *GLv* N. geniculatus lateralis, pars ventralis; *GT* Griseum tectale; *ICO* N. intercollicularis; *Imc* N. isthmi, pars magnocellularis; *ION* N. isthmo-opticus; *Ipc* N. isthmi, pars parvocellularis; *IPS* N. interstitio-praetecto-subpraetectalis; *LM* N. lentiformis mesencephali; *NI* Neostriatum intermedium; *Pam* N. paramedianus; *PAP* N. papillioformis; *PL* N. pontis lateralis; *PM* N. pontis medialis; *PT* N. praetectalis; *PV* N. posteroventralis thalami; *RPO* N. reticularis pontis oralis; *Rt* N. rotundus; *SGC* Stratum griseum centrale; *SLu* N. semilunaris; *SP* N. subpraetectalis; *SRt* N. subrotundus; *T* N. triangularis; *TeO* Tectum opticum; *TI* Tractus tecto-isthmicus; *TPT* Tractus tecto-pontinus; *TR* Tractus tecto-reticularis; *VLT* N. ventrolateralis thalami

Examples are shown in Fig. 1: nucleus praetectalis (Fig. 1.9), nucleus ventralis thalami (Fig. 1.10) and nucleus geniculatus lateralis, pars ventralis (Fig. 1.10). Bilateral labels were found in five brain areas (Table 1). Fig. 1.3 shows the nucleus rotundus of the ipsilateral side, Fig. 1.4 the nucleus rotundus of the contralateral side. Both pictures were taken from one section. Contralateral labels were found in three areas of the brainstem (Table 1) and in the optic tectum.

Transport to the contralateral side was further shown by the labeling of some of the interhemispheric commissures. The decussatio supraoptica ventralis (Fig. 1.1) was particularly heavily labeled. The commissura tectalis and the commissura posterior also showed enhanced grain densities (Fig. 1.2). Fig. 2 shows a coronal section demonstrating, once more, the difference between the labeling of the nucleus rotundus of the ipsi- and contralateral side. In addition, the ectostriatum, the telencephalic end-station of the thalamofugal pathway, was labeled above background on the ipsilateral side, most probably because of transneuronal transport of ^{3}H-proline. The contralateral ectostriatum also showed slightly enhanced labeling.

The complexity of the tectofugal projections obtained in this study is shown diagrammatically in Fig. 3. The connections between the different areas are partly taken from other studies (Robert and Cuenod 1969a, b; Voneida and Mello 1975; Benowitz and Karten 1976; Hunt and Künzle 1976a, b).

The density of grains was counted for the nucleus rotundus on both hemispheres and the relative density of the label was calculated (100% = density of the nucleus rotundus ipsilateral from the tectal injection). The results are depicted in Table 2. As can be seen from this Table, the mean relative density for the contralateral nucleus rotundus is 24.1%. This means that the density of labeled axon terminalis within the contralateral nucle-

Table 2. Mean density of silver grains in the nucleus rotundus obtained by grain counts (*left*) or luminance measurements with the exposure meter (*middle*). *Right side*: luminance measurements of SP/IPS. x=mean; s=standard deviation; percentages with respect to the ipsilateral nucleus rotundus (100%)

Experiment (Bird ID)	Grain counts		Optical density			
	Rt ipsilat.	Rt contralat.	Rt ipsilat.	Rt contralat.	SP/IPS ipsilat.	SP/IPS contralat.
Prol. IV	x=103.4 s=14.21 100%	x=21.75 s=5.66 21.03%	x=179.25 mV s=20.87 100%	x=42.03 mV s=8.60 20.24%	X=185.74 mV s=17.24 103.77%	x=28.83 mV s=4.97 12.57%
Prol. V	x=88.82 s=10.16 100%	x=19.47 s=5.4 21.95%	x=184.65 mV s=28.55 100%	x=48.55 mV s=4.42 21.67%	x=205.70 mV s=30.15 112.14%	x35.94 mV s=2.65 14.41%
Prol. VI	x=42.14 s=8.39 100%	x=12.07 s=4.23 28.64%	x=95.48 mV s=8.86 100%	x=41.43 mV s=3.69 23.42%	x=96.93 mV s=8.62 102.50%	x=40.54 mV s=2.00 22.19%
Prol. VII	x=53.18 s=10.20 100%	x=13.11 s=4.38 24.65%	x=120.02 mV s=11.67 100%	x=38.78 mV s=4.00 19.82%	x=143.40 mV s=18.42 123.08%	x=46.56% s=2.57 27.50%
mean	100%	24.1%	100%	21.29%	110.26%	19.17%

us rotundus is roughly one quarter that of the ipsilateral side.

A slightly lower percentage was obtained by measuring the optical density using the exposure meter of the microscope. By use of this method, the mean density of the radioactively labeled terminals in the contralateral nucleus rotundus amounted to 21.29%, showing again that a substantial amount of tectal neurons project to the contralateral nucleus rotundus. The nucleus subpraetectalis/nucleus interstitio-praetecto-subpraetectalis (SP/IPS) complex was heavily labeled on both sides. The densities were 110.26% ipsilaterally and 19.17% contralaterally, when calculated with the density of the ipsilateral nucleus rotundus as 100% (Table 2). With both measurements, there was no indication of differences between different parts of the ipsilateral or contralateral nucleus rotundus.

Table 3. HRP- and RITC-labeled tectal neurons in birds with injections into the nucleus rotundus. Values without asterisks are total counts, values with asterisks are random from the center of the tecta (means ± SEM)

Experiment (Bird ID)	Number of neurons		
	TeO ipsi	TeO contra	% contra
HRP 1	921	39	4.2
HRP 7	1415	38	2.7
HRP 28	952	7	0.74
HRP 32	1629	18	1.1
RITC I	4516	1373	30.4
RITC III	100.9 ± 2.59*	49.1 ± 2.01*	48.6*
RITC IV	127.0 ± 5.45*	59.7 ± 3.34*	47.0*
RITC V	25.2 ± 1.69*	6.4 ± 0.80*	25.4*

Nucleus rotundus-injections

As the densities of ^{3}H-proline-labels within the nucleus rotundus contralateral to the injection site were much higher than expected from a survey of the literature, we injected the retrograde tracers HRP and RITC into the nucleus rotundus to confirm this finding.

Our experiments demonstrate that there are large differences in the numbers of contralaterally labeled neurons; this is probably caused by the sensitivity of the different tracers. Table 3 shows the results of cell counts within the ipsi- and contralateral tectum opticum after HRP and RITC injections into the nucleus rotundus. The percentage of contralateral neurons ranges between 0.74% and 4.2% of the number of neurons labeled on the ipsilateral side in HRP-injected animals. On the other hand, RITC injections reveal a much larger number of labeled neurons on both the ipsi- and on the contralateral side. In contrast to the HRP-experiments, the percentage of neurons labeled on the contralateral side ranges from 25.4 to 48.6% depending on the size of the injection. This is even higher than the percentage obtained by anterograde labeling with ^{3}H-proline. This difference between the methods can be seen in photographs of the ipsi- and contralateral tectum (Fig. 1.5–1.8).

In addition, injections into the nucleus rotundus revealed labels within the nucleus subpraetectalis/nucleus interstitio-praetecto-subpraetectalis (SP/IPS) complex and within a nucleus that could not be clearly identified. Most probably, this nucleus was the nucleus decussationis supraopticae ventralis (ND, Reperant 1973). In one case, a few labeled neurons were found within the contralateral nucleus rotundus. We did not find a clear relation between the site of the injection and the distribution of labeled neurons within the tectum opticum. At best, there was a tendency that ipsilaterally more neurons were labeled in the dorsal part of the tectum, whereas the neurons on the contralateral side were slightly

more concentrated in the ventral part of the stratum griseum centrale.

RITC injections, optic tectum

The ^{3}H-proline injections also resulted in a very low labeling of the contralateral tectum opticum, indicating that the tectum-tectum projection is small. We injected RITC into the tectum opticum to confirm this. In agreement with our anterograde tracing results, these injections showed that only a very small number of neurons can be found in the contralateral tectum. This cannot be the result of low sensitivity of the RITC method, since this method has been shown to be very sensitive by our nucleus rotundus-injections. Our results strongly suggest that the tectum-tectum projection in the zebra finch is much smaller than the projection between tectum opticum and the contralateral nucleus rotundus.

Discussion

Our results demonstrate that the optic tectum is one of the major relay stations in the avian brain; it projects to a variety of visual areas, and to acoustic, somatosensory and other areas of as yet unknown function (Harmon and Phillips 1967; Karten 1967; Delius and Bennetto 1972; Knudsen and Knudsen 1983). Studies with retrograde tracers (Niemann and Bischof in preparation; Bagnoli et al. 1980; Reiner et al. 1982; Henke 1983) show that there is also multiple input to the tectum opticum.

In this discussion, however, we will concentrate on the connections with the contralateral hemisphere because the examination of these connections was the main aim of our experiment. As mentioned in the introductory section, the "classical" view of information processing within the visual system of birds is that the thalamofugal pathway is involved in processing information from the binocular visual field (Pettigrew and Konishi 1976; Wilson 1980a, b; Pettigrew 1977), whereas the tectofugal pathway is mainly involved in the processing of the contralateral monocular visual field (Revzin and Karten 1966/67; Revzin 1970; Kimberly et al. 1971; Parker and Delius 1972; Mori 1973).

Studies from our laboratory, however, have demonstrated that the tectofugal pathway also processes data from the ipsilateral eye (for review, see Bischof 1989). Therefore, it is likely that the tectofugal pathway is involved in binocular vision. As the optic nerve in adult birds crosses completely to the contralateral side (see Cowan et al. 1961), recrossing projections between the two hemispheres must be present. Such projections from the optic tectum have been demonstrated in the pigeon by several authors. The areas found to receive recrossing tectal projections are the tectum opticum, the nucleus rotundus, the nucleus subpraetectalis, the nucleus interstitio-praetecto-subpraetectalis, area praetectalis, and nucleus geniculatus lateralis, pars ventralis (Hunt and Kuenzle 1976a; Robert and Cuenod 1969a, b; Voneida and Mello 1975; Benowitz and Karten 1976). The information obtained from these studies, however, is not very uniform. For example, Voneida and Mello (1975), on the basis of degeneration studies, could not demonstrate recrossing tecto-rotundal projections. However, Benowitz and Karten (1976) have demonstrated using HRP injections that a small recrossing tecto-rotundal projection exists. In contrast, autoradiographic studies with the anterograde tracer ^{3}H-proline indicate that this projection is massive (Hunt and Kuenzle 1976a, b). Because we suspected (Engelage and Bischof 1988) that the tecto-rotundal projection may be very important for ipsilateral stimulus processing, we have tried to estimate the number of tecto-rotundal fibers in the zebra finch quantitatively by the use of different methods.

Our results suggest that the large variation obtained in the studies mentioned above probably results from the different techniques used. We also find a much smaller ipsi/contra percentage in the HRP studies than in those involving ^{3}H-proline. The neurons that project to the contralateral nucleus rotundus may have very strongly aborized axons; this would lead to an enhanced labeling of terminals within the nucleus rotundus in spite of the small number of neurons projecting from the tectum to the nucleus rotundus. However, our RITC injections into the nucleus rotundus reveal that the small amount of labeled neurons obtained with HRP may be a result of a lower efficiency of this method in demonstrating contralateral projections, when compared with the anterograde tracing technique using radioactive proline, or with the application of the retrograde tracer RITC. At present, we are unable to explain this conspicuous differences. It is unlikely that the difference is caused, for example, by different size of the injection, or extent of diffusion, as these were similar in both the RITC and the HRP experiments. Moreover, even a very circumscribed injection of RITC located at the dorsal border of rotundus (experiment RITC V, Table 3) causes a percentage of contralaterally labeled neurons of 25.4%, which is much larger than the values obtained with the use of HRP. This experiment shows that the size of the injection has influence on the number of labeled neurons, but not on the percentage of contralaterally labeled cells.

Even if the percentage values of contralateral labeling may be overestimated in the RITC preparations, because the ipsilateral counts may be too low as a consequence of the high density of neurons on this side, our results show that the projection from the tectum opticum to the nucleus rotundus is much stronger than previously thought. In contrast, we have confirmed the finding that the tecto-tectal projection is very weak. Even with RITC injections into the optic tectum only a few, quite weakly labeled neurons can be found within the contralateral tectum.

We presume that, in the zebra finch, the most important pathway for the processing of stimuli from the ipsilateral eye is the projection from the optic tectum to the contralateral nucleus rotundus. This is supported by our electrophysiological data (Engelage and Bischof 1988). In this study, we found only very weak responses

to ipsilateral stimulation within the optic tectum, even in unilaterally enucleated birds, where the ipsilateral response of the ectostriatum was drastically enhanced by removal of the contralateral eye. In addition to the tectorotundal projection, the recrossing tecto-IPS/SP projection may contribute to the processing of ipsilateral stimuli, as these two nuclei are also heavily labelled in our study. Recent results from Shimizu et al. (1988) have provided evidence that these nuclei, which in turn project to the ipsilateral nucleus rotundus, mediate inhibitory effects. However, as the two nuclei also receive input from the ipsilateral tectum, it is not yet clear whether this inhibition mainly stems from ipsi- or contralateral information, or from both.

Acknowledgements. Our thanks are due to Dr. Nicky Clayton, who improved the English text, and to Edda Geißler who provided excellent technical assistence. Financial support came from the Deutsche Forschungsgemeinschaft (Bi245/4).

References

Bagnoli P, Grassi S, Magni F (1980) A direct connection between visual wulst and tectum opticum in the pigeon (*Columba livia*) demonstrated by horseradish peroxidase. Arch Ital Biol 118:72–88

Benowitz L, Karten HJ (1976) The organization of the tectofugal pathway in the pigeon: a retrograde transport study. J Comp Neurol 167:503–520

Bischof HJ (1981) A stereotaxic headholder for small birds. Brain Res Bull 7:435–436

Bischof HJ (1989) Neuronal plasticity in the development of birds. In: Rahmann H, Lindauer M (eds) Fundamentals of memory formation: neuronal plasticity and brain function. Fortschritte der Zoologie 37, Fischer Verlag, Stuttgart:115–131

Cowan WM, Adamson L, Powell TPS (1961) An experimental study of the avian visual system. J Anat 95:545–563

Delius JD, Bennetto K (1972) Cutaneous sensory projections to the avian forebrain. Brain Res 37:205–221

Engelage J, Bischof HJ (1988) Enucleation enhances ipsilateral flash responses in the ectostriatum of the zebra finch (*Taenopygia guttata castanotis* Gould). Exp Brain Res 70:79–89

Engelage J, Bischof HJ (1989) Flash evoked potentials in the ectostriatum of the zebra finch: a current source-density analysis. Exp Brain Res 74:563–572

Harmon AL, Phillips RE (1967) Responses in the avian midbrain, thalamus and forebrain evoked by click stimuli. Exp Neurol 18:276–286

Henke H (1983) The central part of the avian visual system. In: Nistico G, Bolis L (eds) Progress in mammalian brain research Vol I, CRC Press, Boca Raton, Florida, pp 113–158

Herrmann K, Bischof HJ (1986a) Effects of monocular deprivation in the nucleus rotundus of zebra finches: a deoxyglucose and Nissl study. Exp Brain Res 64:119–126

Herrmann K, Bischof HJ (1986b) Monocular deprivation affects neuron size in the ectostriatum of the zebra finch brain. Brain Res 379:143–146

Hunt SP, Künzle H (1976a) Observations of the pigeon optic tectum: an autoradiographic study based on anterograde and retrograde, axonal and dendritic flow. J Comp Neurol 170:153–172

Hunt SP, Künzle H (1976b) Selective uptake and transport of label within three identified neuronal systems after injections of (^{3}H)-GABA into the pigeon optic tectum: an autoradiographic and Golgi study. J Comp Neurol 170:175–189

Karten HJ (1967) The organization of the ascending auditory pathway in the pigeon (*Columba livia*) I. Diencephalic projections of the inferior colliculus (nucleus mesencephali lateralis, pars dorsalis). Brain Res 6:409–427

Karten HJ, Hodos W (1967) A stereotaxic atlas of the brain of the pigeon (*Columba livia*). Johns Hopkins University Press, Baltimore

Kimberly RP, Holden AL, Barmborough P (1971) Response characteristics of pigeon forebrain cells to visual stimulation. Vision Res 11:475–478

Knudsen EI, Knudsen PF (1983) Space-mapped auditory projections from the inferior colliculus to the optic tectum in the barn owl (*Tyto alba*). J Comp Neurol 218:187–196

McLoon SC, Lund RP (1982) Transient retinofugal pathways in the developing chick. Exp Brain Res 34:277–284

Mesulam MM (1978) Tetramethyl benzidine for horseradish peroxidase histochemistry: A non carcinogenic blue reaction product with superior sensitivity for visualizing neural afferents and efferents. J Histochem Cytochem 26:106–117

Mori S (1973) Analysis of field response in optic tectum of the pigeon. Brain Res 54:193–206

Nixdorf B, Bischof HJ (1987) Ultrastructural effects of monocular deprivation in the neuropil of nucleus rotundus in the zebra finch: a quantitative electron microscopic study. Brain Res 405:326–336

O'Leary DDM, Gerfen ChR, Cowan M (1983) The development and restriction of the ipsilateral retinofugal projection in the chick. Dev Brain Res 10:93–109

Parker DM, Delius JD (1972) Visual evoked potentials in the forebrain of the pigeon. Exp Brain Res 14:198–209

Pettigrew JD (1977) Comparison of the retinotopic organization of the visual wulst in nocturnal and diurnal raptors, with a note on the evolution of frontal vision. In: Cool SJ, Smith EL (eds) Frontiers in visual science. Springer, Berlin Heidelberg New York, pp 328–333

Pettigrew JD, Konishi M (1976) Neurons selective for orientation and binocular disparity in the visual wulst of the barn owl (*Tyto alba*). Science 193:675–678

Reiner A, Brecha NC, Karten HJ (1982) Basal ganglia pathways to the tectum: the afferent and efferent connections of the lateral spiriform nucleus of the pigeon. J Comp Neurol 208:16–36

Reperant J (1973) Nouvelles donneés sur les projections visuelles chez le pigeon (*Columba livia*). J Hirnforsch 14:152–187

Revzin AM (1970) Some characteristics of wide field units in the pigeon brain. Brain Behav Evol 3:195–204

Revzin AM, Karten HJ (1966/67) Rostral projections of the optic tectum and nucleus rotundus in the pigeon. Brain Res 3:244–276

Robert F, Cuenod M (1969a) Electrophysiology of the intertectal commissures in the pigeon. I. Analysis of the pathways. Exp Brain Res 9:116–122

Robert F, Cuenod M (1969b) Electrophysiology of the intertectal commissures in the pigeon. II. Inhibitory interaction. Exp Brain Res 9:123–136

Shimizu T, Karten HJ, Woodson W (1988) GABAergic inputs to the nucleus rotundus in pigeon (*Columba livia*). Soc Neurosci [Abstr] 1988, 397.9

Stokes TM, Leonhard CM, Nottebohm F (1972) The telencephalon, diencephalon and mesencephalon of the canary, *Serinus canaria*, in stereotaxic coordinates. J Comp Neurol 156:337–374

Voneida TJ, Mello NK (1975) Interhemispheric projections of the optic tectum in the pigeon. Brain Behav Evol 11:91–108

Weidner C, Reperant J, Miceli D, Haby M, Rio JP (1985) An anatomical study of ipsilateral retinal projections in the quail using autoradiography, HRP, fluorescence and degeneration techniques. Brain Res 340:99–108

Wilson P (1980a) The organization of the visual hyperstriatum in the domestic chick. I. Topology and topography of the visual projection. Brain Res 188:319–332

Wilson P (1980b) The organization of the visual hyperstriatum in the domestic chick. II. Receptive field properties of single units. Brain Res 188:333–345